Isospin Diffusion in Thermal AdS/CFT Correspondence with Flavor

Johanna Erdmenger – Werner-Heisenberg Institut

Matthias Kaminski – Werner-Heisenberg Institut

Felix Rust – Werner-Heisenberg Institut

Citation of published version:

Erdmenger, J., Kaminski, M., Rust, F. (2007): Isospin Diffusion in Thermal AdS/CFT Correspondence with Flavor, *Physical Review D 76*. http://dx.doi.org/10.1103/PhysRevD.76.046001

PHYSICAL REVIEW D **76,** 046001 (2007)

Isospin diffusion in thermal AdS/CFT correspondence with flavor

Johanna Erdmenger,* Matthias Kaminski,† and Felix Rust‡

Max-Planck-Institut für Physik (Werner-Heisenberg-Institut), Föhringer Ring 6, 80805 München, Germany

(Received 24 April 2007; published 2 August 2007)

We study the gauge/gravity dual of a finite temperature field theory at finite isospin chemical potential by considering a probe of two coincident D7-branes embedded in the AdS-Schwarzschild black hole background. The isospin chemical potential is obtained by giving a vacuum expectation value to the time component of the non-Abelian gauge field on the brane. The fluctuations of the non-Abelian gauge field on the brane are dual to the $SU(2)$ flavor current in the field theory. For the embedding corresponding to vanishing quark mass, we calculate all Green functions corresponding to the components of the flavor current correlator. We discuss the physical properties of these Green functions, which go beyond linear response theory. In particular, we show that the isospin chemical potential leads to a frequency-dependent isospin diffusion coefficient.

DOI: 10.1103/PhysRevD.76.046001 PACS numbers: 11.25.Tq, 11.10.Wx, 11.25.Wx, 12.38.Mh

I. INTRODUCTION

Over the past years, there have been a number of lines of investigation for describing QCD-like theories with gravity duals. In this way, considerable progress towards a gauge/gravity dual description of phenomenologically relevant models has been made. One of these lines of investigation is the gravity dual description of the quark-gluon plasma obtained by applying AdS/CFT to relativistic hydrodynamics [1–7]. The central result of this approach is the calculation of the shear viscosity from AdS/CFT. More recently, an R charge chemical potential has been introduced by considering gravity backgrounds with R charged black holes [8–10], and also the heat conductivity has been calculated by considering the R current correlators in these backgrounds [8].

A further approach to generalizing the AdS/CFT correspondence to more realistic field theories is the addition of flavor to gravity duals via the addition of probe branes [11–15]. This allows, in particular, for the calculation of meson masses.

These two approaches have been combined in order to study the flavor contribution to finite temperature field theories from the gravity dual perspective. This began with [13] where the embedding of a D7-brane probe into the AdS-Schwarzschild black hole background was studied and a novel phase transition was found, which occurs when the D7 probe reaches the black hole horizon. This transition was shown to be of first order in [16] (see [14] for a similar transition in the D4/D6 system), and studied in further detail in [17,18]. Related phase transitions appear in [19–21]. Mesons in gravity duals of finite temperature field theories have been studied in [22–25].

Recently, in view of adding flavor to the quark-gluon plasma, the flavor contribution to the shear viscosity has been calculated in [26,27], where it was found that $\eta_{\text{fund}} \propto \lambda N_c N_f T^3$.

For a thermodynamical approach in the grand canonical ensemble, the inclusion of a chemical potential and a finite number density are essential. In [28], an isospin chemical potential was introduced by considering two coincident D7 probes, and by giving a vacuum expectation value (VEV) to the time component of the $SU(2)$ gauge field on this probe. This was shown to give rise to a thermodynamical instability comparable to Bose-Einstein condensation, compatible with the field-theoretical results of [29]. For the gauge/gravity dual analysis, a potential generated by an $SU(2)$ instanton on the D7 probe in the gravity background was used [30–33].

A baryon chemical potential μ_B is obtained by turning on the diagonal $U(1) \subset U(N_f)$ gauge field on the D7-brane probe [34]. Contributions to the D7-brane action arise from the derivative of this $U(1)$ gauge field with respect to the radial direction. The effects of this potential on the first-order phase transition described above have been studied in [34], where regions of thermodynamical instability have been found in the (T, μ_B) phase diagram. For the $D4/D8/\bar{D}8$ Sakai-Sugimoto model [15,35], the phase transitions in presence of a baryon number chemical potential, as well as physical processes such as photoemission and vector meson screening, have been studied in [36–38].

A related approach has been used to calculate the rate of energy loss of a heavy quark moving through a supersymmetric Yang-Mills plasma at large coupling [39]. In this approach the heavy quark is given by a classical string attached to the D7-brane probe. A first study of flavors in thermal AdS/CFT beyond the quenched approximation, i.e. with $N_f \sim N_c$, was performed in [40].

Here we study finite temperature field theories with finite isospin chemical potential by considering two coincident D7-brane probes in the Lorentzian signature AdS-Schwarzschild black hole background. As in [28], we introduce an isospin chemical potential by defining

*jke@mppmu.mpg.de
†kaminski@mppmu.mpg.de
‡rust@mppmu.mpg.de

$$A_0 = \begin{pmatrix} \mu & 0 \\ 0 & -\mu \end{pmatrix}, \tag{1.1}$$

for the time component of the $SU(2)$ gauge field on the two coincident D7-branes. This constant chemical potential is a solution to the D7-brane equations of motion and is present even for the D7-brane embedding corresponding to massless quarks. We consider small μ, such that the Bose-Einstein instability mentioned above, which is of order $\mathcal{O}(\mu^2)$, does not affect our discussion here.

For simplicity we consider only the D7 probe embedding for which the quark mass vanishes, $m = 0$. This embedding is constant and terminates at the horizon. We establish the $SU(2)$ non-Abelian action for a probe of two coincident D7-branes. We obtain the equations of motion for fluctuations about the background given by (1.1). These are dual to the $SU(2)$ flavor current $J^{\mu a}$. We find an ansatz for decoupling the equations of motion for the different Lorentz and flavor components, and solve them by adapting the method developed in [2,3]. This involves Fourier transforming to momentum space, and using a power expansion ansatz for the equations of motion. We discuss the approximation necessary for an analytical solution, which amounts to considering frequencies with $\omega < \mu < T$. With this approach we obtain the complete current-current correlator. The key point is that the constant chemical potential effectively replaces a time derivative in the action and in the equations of motion. In the Fourier transformed picture, this leads to a square-root dependence of physical observables on the frequency, $\sqrt{\omega}$. This nonlinear behavior goes beyond linear response theory. We discuss the physical properties of the Green functions contributing to the current-current correlator. In particular, for small frequencies we find a frequency-dependent diffusion coefficient $D(\omega) \propto \frac{1}{T}\sqrt{\omega/\mu}$. Whereas frequency-dependent diffusion has—to our knowledge—not yet been discussed in the context of the quark-gluon plasma, it is well-known in the theory of quantum liquids. For instance, for small frequencies the square-root behavior we find agrees qualitatively with the results of [41,42] for liquid parahydrogen. Generally, frequency-dependent diffusion leads to a nonexponential decay of time-dependent fluctuations, as discussed for a classical fluid in [43].

Physically, the isospin chemical potential corresponds to the energy necessary to inverting the isospin of a given particle. Within nuclear physics, such a chemical potential is of relevance for the description of neutron stars. Moreover, isospin diffusion has been measured in heavy ion reactions [44,45]. For two-flavor QCD, effects of a finite isospin chemical potential have been discussed for instance in [46–48]. The phase diagrams discussed there are beyond the scope of the present paper. We expect to return to similar diagrams in the gauge/gravity dual context in the future.

This paper is organized as follows. In Sec. II we summarize the AdS/CFT hydrodynamics approach to calculating Green functions, which we use in the subsequent sections. Moreover we comment on frequency-dependent diffusion within hydrodynamics. In Sec. III we establish the D7 probe action in presence of the isospin chemical potential, derive the corresponding equations of motion and solve them. In Sec. IV we obtain the associated Green functions in the hydrodynamical approximation. We discuss their pole structure and obtain the frequency-dependent diffusion coefficient. We conclude in Sec. V with an interpretation of our results. An explanation of our notation as well as a series of calculations are relegated to a number of appendices.

II. HYDRODYNAMICS AND ADS/CFT

Thermal Green functions have proven to be a useful tool for analyzing the structure of hydrodynamic theories and for calculating hydrodynamic quantities such as transport coefficients. For instance, given a retarded current correlation function $G(\vec{k})_{\mu\nu}$ in Minkowski space, the spectral function can be written in terms of its imaginary part,

$$\chi_{\mu\nu}(\vec{k}) = -2\,\mathrm{Im} G_{\mu\nu}(\vec{k}). \tag{2.1}$$

For the gravity dual approach, this is discussed for instance in [7,49].

In this paper we use the gauge/gravity dual prescription of [3] for calculating Green functions in Minkowski spacetime. For further reference, we outline this prescription in the subsequent. It is based on the AdS/CFT correspondence relating supergravity fields A in a black hole background to operators J in the dual gauge theory. The black hole background is asymptotically Anti-de Sitter space and places the dual field theory at finite temperature. This temperature corresponds to the Hawking temperature of the black hole, or more generally speaking, of the black branes. Starting out from a classical supergravity action S_{cl} for the gauge field A, according to [3] we extract the function $B(u)$ (containing metric factors and the metric determinant) in front of the kinetic term $(\partial_u A)^2$,

$$S_{\mathrm{cl}} = \int \mathrm{d}u \mathrm{d}^4x\, B(u)(\partial_u A)^2 + \ldots. \tag{2.2}$$

Then we perform a Fourier transformation and solve the linearized equations of motion in momentum space. This is a second-order differential equation, so we have to fix two boundary conditions. The first one at the boundary of AdS at $u = 0$ can be written as

$$A(u, \vec{k}) = f(u, \vec{k}) A^{\mathrm{bdy}}(\vec{k}), \tag{2.3}$$

where $A^{\mathrm{bdy}}(\vec{k})$ is the value of the supergravity field at the boundary of AdS depending only on the four flat boundary coordinates. Thus by definition we have $f(u, \vec{k})|_{u\to 0} = 1$. For the other boundary, located at the horizon $u = 1$, we impose the incoming wave condition. This requires that any Fourier mode $A(\vec{k})$ with timelike $\vec{k}$ can travel into the

black hole, but is not allowed to cross the horizon in the opposite direction. For spacelike $\vec{k}$, the components of A have to be regular at the horizon. Then the retarded thermal Green function is given by

$$G(\omega, \boldsymbol{k}) = 2B(u)f(u, -\vec{k})\partial_u f(u, \vec{k})|_{u\to 0}. \tag{2.4}$$

The thermal correlators obtained in this way display hydrodynamic properties, such as poles located at complex frequencies. Generically, for the R current component correlation functions calculated from supergravity, there are retarded contributions of the form

$$G(\omega, \boldsymbol{k}) \propto \frac{1}{i\omega - D\boldsymbol{k}^2}. \tag{2.5}$$

This may be identified with the Green function for the hydrodynamic diffusion equation

$$\partial_0 J_0(t, \boldsymbol{x}) = D\nabla^2 J_0(t, \boldsymbol{x}), \tag{2.6}$$

with J_0 the time component of a diffusive current. D is the diffusion constant. In Fourier space this equation reads

$$i\omega J_0(\omega, \boldsymbol{k}) = D\boldsymbol{k}^2 J_0(\omega, \boldsymbol{k}). \tag{2.7}$$

In position space, this corresponds to an exponential decay of J_0 with time.

For the non-Abelian case with an isospin chemical potential, in Secs. III and IV we will obtain retarded Green functions of the form

$$G(\omega, \boldsymbol{k}) \propto \frac{1}{i\omega - D(\omega)\boldsymbol{k}^2}. \tag{2.8}$$

Retarded Green functions of this type have been discussed for instance in [43]. Equation (2.8) corresponds to frequency-dependent diffusion with coefficient $D(\omega)$, such that (2.7) becomes

$$i\omega J_0(\omega, \boldsymbol{k}) = D(\omega)\boldsymbol{k}^2 J_0(\omega, \boldsymbol{k}). \tag{2.9}$$

In our case, J_0 is the averaged isospin at a given point in the liquid.

This is a nonlinear behavior which goes beyond linear response theory. In particular, when Fourier transforming back to position space, we have to use the convolution for the product $D \cdot J_0$ and obtain

$$\partial_0 J_0(t, \boldsymbol{x}) + \nabla^2 \int_{-\infty}^{t} \mathrm{d}s J_0(s, \boldsymbol{x}) D(t - s) = 0 \tag{2.10}$$

for the retarded Green function. This implies together with the continuity equation $\partial_0 J_0 + \boldsymbol{\nabla} \cdot \boldsymbol{J} = 0$, with $\boldsymbol{J}$ the three-vector current associated to J_0, that

$$\boldsymbol{J} = -\boldsymbol{\nabla}(D * J_0), \tag{2.11}$$

where $*$ denotes the convolution. This replaces the linear response theory constitutive equation $\boldsymbol{J} = -D\boldsymbol{\nabla} J_0$. Note that for $D(t - s) = D\delta(t - s)$ with D constant, (2.10) reduces again to (2.6).

III. SUPERGRAVITY BACKGROUND AND ACTION

A. Finite temperature background and brane configuration

We consider an asymptotically $\mathrm{AdS}_5 \times S^5$ spacetime as the near horizon limit of a stack of N_c coincident D3-branes. More precisely, as in [2], our background is an AdS black hole, which is the geometry dual to a field theory at finite temperature. The Minkowski signature background is

$$\begin{aligned} \mathrm{d}s^2 &= \frac{b^2R^2}{u}(-f(u)\mathrm{d}x_0^2 + \mathrm{d}x_1^2 + \mathrm{d}x_2^2 + \mathrm{d}x_3^2) \\ &\quad + \frac{R^2}{4u^2 f(u)}\mathrm{d}u^2 + R^2\mathrm{d}\Omega_5^2, \\ 0 \le u \le 1, &\qquad x_i \in \mathbb{R}, \qquad C_{0123} = \frac{b^4R^4}{u^2}, \end{aligned} \tag{3.1}$$

with the metric $\mathrm{d}\Omega_5^2$ of the unit 5-sphere, and the function $f(u)$, AdS radius R and temperature parameter b given in terms of the string coupling g_s, temperature T, inverse string tension α' and number of colors N_c by

$$f(u) = 1 - u^2, \qquad R^4 = 4\pi g_s N_c \alpha'^2, \qquad b = \pi T. \tag{3.2}$$

The geometry is asymptotically $\mathrm{AdS}_5 \times S^5$ with the boundary of the AdS part located at $u = 0$. At the black hole horizon the radial coordinate u has the value $u = 1$.

Into this ten-dimensional spacetime we embed $N_f = 2$ coinciding D7-branes, hosting flavor gauge fields A_μ. The embedding we choose extends the D7-branes in all directions of AdS space and wraps an S^3 on the S^5. In this work we restrict ourselves to the most straightforward case, that is the embedding of the branes through the origin along the AdS radial coordinate u. This corresponds to massless quarks in the dual field theory. On the brane, the metric in this case simply reduces to

$$\begin{aligned} \mathrm{d}s^2 &= \frac{b^2R^2}{u}(-f(u)\mathrm{d}x_0^2 + \mathrm{d}x_1^2 + \mathrm{d}x_2^2 + \mathrm{d}x_3^2) \\ &\quad + \frac{R^2}{4u^2 f(u)}\mathrm{d}u^2 + R^2\mathrm{d}\Omega_3^2, \\ 0 \le u \le 1, &\qquad x_i \in \mathbb{R}. \end{aligned} \tag{3.3}$$

Due to the choice of our gauge field in the next subsection, the remaining 3-sphere in this metric will not play a prominent role.

The table below gives an overview of the indices we use to refer to certain directions and subspaces.

	AdS_5					S^3
coord. names	x^0	x^1	x^2	x^3	u	–
	$\mu, \nu \ldots$					
indices	$i, j \ldots$				u	
	α					

B. Introducing a non-Abelian chemical potential

A gravity dual description of a chemical potential amounts to a nondynamical time component of the gauge field A_μ in the action for the D7-brane probe embedded into the background given above. There are essentially two different ways to realize a nonvanishing contribution from a chemical potential to the field strength tensor $F = 2\partial_{[\mu}A_{\nu]} + f^{abc}A^b_\mu A^c_\nu$. The first is to consider a u-dependent baryon chemical potential for a single brane probe. The second, which we pursue here, is to consider a constant isospin chemical potential. This requires a non-Abelian probe brane action and thus a probe of at least two coincident D7-branes, as suggested in [28]. Here the time component of the gauge field is taken to be

$$A_0 = A^a_0 t^a, \tag{3.4}$$

where we sum over indices which occur twice in a term and denote the gauge group generators by t^a. The brane configuration described above corresponds to an $SU(N_f)$ gauge group with $N_f = 2$ on the brane, which corresponds to a global $SU(N_f)$ in the dual field theory. For $N_f = 2$, the generators of the gauge group on the brane are given by $t^a = \frac{\sigma^a}{2}$, with Pauli matrices σ^a. We will see that (3.4) indeed produces nontrivial new contributions to the action.

Using the standard background field method of quantum field theory, we will consider the chemical potential as a fixed background and let the gauge fields fluctuate. We single out a particular direction in flavor space by taking $A^3_0 = \mu$ as the only nonvanishing component of the background field. From now on we use the symbol A^a_ν to refer to gauge field fluctuations around the fixed background,

$$A^a_\nu \rightarrow \mu\delta_{\nu 0}\delta^{a3} + A^a_\nu. \tag{3.5}$$

We pick the gauge in which $A_u \equiv 0$ and assume that $A_\mu \equiv 0$ for $\mu = 5, 6, 7$. Because of the symmetries of the background, we effectively examine gauge field fluctuations A_μ living in the five-dimensional subspace on the brane spanned by the coordinates x_0, x_1, x_2, x_3 and by the radial AdS coordinate u. The magnitude of all components of A and the background chemical potential μ are considered to be small. This allows us to simplify certain expressions by dropping terms of higher order in A and in the chemical potential μ.

C. Dirac-Born-Infeld action

The action describing the dynamics of the flavor gauge fields in the setup of this work is the Dirac-Born-Infeld (DBI) action. There are no contributions from the Chern-Simons action, which would require nonzero gauge field components in all of the 4, 5, 6, 7-directions. As mentioned, we consider the D7 probe embedding whose asymptotic value at the boundary is chosen such that it corresponds to vanishing quark mass, $m = 0$. The metric on the brane is then given by (3.3). Since we are interested in two-point correlators only, it is sufficient to consider the action to second order in α',

$$S_{\mathrm{D7}} = -T_7\frac{(2\pi\alpha')^2}{2}2\pi^2R^3T_r\int_{u_b=0}^{u_h=1}\mathrm{d}u\mathrm{d}^4x\sqrt{-g}g^{\mu\mu'} \times g^{\nu\nu'}F^a_{\mu\nu}F^a_{\mu'\nu'}, \tag{3.6}$$

where we use the following definitions for the D7-brane tension T_7 and the trace over the representation matrices t^a,

$$T_7 = (2\pi)^{-7}g_s^{-1}(\alpha')^{-4}, \tag{3.7}$$

$$\mathrm{tr}\,(t^at^b) = T_r\delta^{ab}. \tag{3.8}$$

In our case we have $T_r = 1/2$. The overall factor $2\pi^2R^3$ comes from the integration over the 5, 6, 7-directions, which are the directions along the S^3.

Evaluating the DBI action given in (3.6) with the substitution rule (3.5), we arrive at

$$S_{\mathrm{D7}} = -T_7\frac{(2\pi\alpha')^2}{2}2\pi^2R^3T_r\int_{u_b=0}^{u_h=1}\mathrm{d}u\mathrm{d}^4x\sqrt{-g}g^{\mu\mu'} \times g^{\nu\nu'}(4\partial_{[\mu}A^a_{\nu]}\partial_{[\mu'}A^a_{\nu']} - 8\delta_{0\nu}\delta_{0\nu'}f^{abc}\partial_{[0}A^a_{\mu]}A^b_{\mu'}\mu^c), \tag{3.9}$$

where we use the short-hand notation $\mu^c = \mu\delta^{3c}$ and neglect terms of higher than linear order in μ, and higher than quadratic order in A since both are small in our approach.

Up to the sum over flavor indices a, the first term in the bracket in (3.9) is reminiscent of the Abelian super-Maxwell action in five dimensions, considered already for the R charge current correlators in [2]. The new second term in our action arises from the non-Abelian nature of the gauge group, giving terms proportional to the gauge group's structure constants f^{abc} in the field strength tensor $F^a_{\mu\nu} = 2\partial_{[\mu}A^a_{\nu]} + f^{abc}A^b_\mu A^c_\nu$.

D. Equations of motion

We proceed by calculating the retarded Green functions for the action (3.9), following the prescription of [3] as outlined in Sec. II above. According to this prescription, as a first step we consider the equations of motion obtained from the action (3.9), which are given by

$$0 = 2\partial_\mu(\sqrt{-g}g^{\mu\mu'}g^{\nu\nu'}\partial_{[\mu'}A^a_{\nu']}) + f^{abc}[\sqrt{-g}g^{00}g^{\nu\nu'}\mu^c(\partial_{\nu'}A^b_0 - 2\partial_0 A^b_{\nu'}) + \delta^{0\nu}\partial_\mu(\sqrt{-g}g^{00}g^{\mu\mu'}A^b_{\mu'}\mu^c)]. \quad (3.10)$$

It is useful to work in momentum space from now on. We therefore expand the bulk gauge fields in Fourier modes in the x^i directions,

$$A_\mu(u,\vec{x}) = \int \frac{\mathrm{d}^4k}{(2\pi)^4} e^{-i\omega x_0 + i\vec{k}\cdot\vec{x}} A_\mu(u,\vec{k}). \quad (3.11)$$

As we work in the gauge where $A_u = 0$, we only have to take care of the components A_i with $i = 0, 1, 2, 3$.

For the sake of simplicity, we choose the momentum of the fluctuations to be along the x_3 direction, so their momentum four-vector is $\vec{k} = (\omega, 0, 0, q)$. With this choice we have specified to gauge fields which only depend on the radial coordinate u, the time coordinate x_0 and the spatial x_3 direction.

1. Equations for A^a_1- and A^a_2-components

Choosing the free Lorentz index in the equations of motion (3.10) to be $\nu = \alpha = 1, 2$ gives two identical differential equations for A_1 and A_2,

$$0 = A^{a\prime\prime}_\alpha + \frac{f'}{f}A^{a\prime}_\alpha + \frac{\mathfrak{w}^2 - f\mathfrak{q}^2}{uf^2}A^a_\alpha + 2i\frac{\mathfrak{w}}{uf^2}f^{abc}\frac{\mu^b}{2\pi T}A^c_\alpha, \quad (3.12)$$

where we indicated the derivative with respect to u with a prime and have introduced the dimensionless quantities

$$\mathfrak{w} = \frac{\omega}{2\pi T}, \qquad \mathfrak{q} = \frac{q}{2\pi T}, \qquad \mathfrak{m} = \frac{\mu}{2\pi T}. \quad (3.13)$$

We now make use of the structure constants of $SU(2)$, which are $f^{abc} = \varepsilon^{abc}$, where ε^{abc} is the totally antisymmetric epsilon symbol with $\varepsilon^{123} = 1$. Writing out (3.12) for the three different choices of $a = 1, 2, 3$ results in

$$0 = A^{1\prime\prime}_\alpha + \frac{f'}{f}A^{1\prime}_\alpha + \frac{\mathfrak{w}^2 - f\mathfrak{q}^2}{uf^2}A^1_\alpha - 2i\frac{\mathfrak{m}\mathfrak{w}}{uf^2}A^2_\alpha, \quad (3.14)$$

$$0 = A^{2\prime\prime}_\alpha + \frac{f'}{f}A^{2\prime}_\alpha + \frac{\mathfrak{w}^2 - f\mathfrak{q}^2}{uf^2}A^2_\alpha + 2i\frac{\mathfrak{m}\mathfrak{w}}{uf^2}A^1_\alpha, \quad (3.15)$$

$$0 = A^{3\prime\prime}_\alpha + \frac{f'}{f}A^{3\prime}_\alpha + \frac{\mathfrak{w}^2 - f\mathfrak{q}^2}{uf^2}A^3_\alpha. \quad (3.16)$$

The first two of these equations are coupled, the third one is the same equation that was solved in the Abelian super-Maxwell case [2].

2. Equations for A^a_0- and A^a_3-components

The remaining choices for the free Lorentz index $\nu = 0$, 3, u in (3.10) result in three equations which are not independent. The choices $\nu = 0$ and $\nu = u$ give

$$0 = A^{a\prime\prime}_0 - \frac{\mathfrak{q}^2}{uf}A^a_0 - \frac{\mathfrak{q}\mathfrak{w}}{uf}A^a_3 - i\frac{\mathfrak{q}}{uf}f^{abc}\frac{\mu^b}{2\pi T}A^c_3, \quad (3.17)$$

$$0 = \mathfrak{w}A^{a\prime}_0 + \mathfrak{q}fA^{a\prime}_3 + if^{abc}\frac{\mu^b}{2\pi T}A^{c\prime}_0. \quad (3.18)$$

Solving (3.18) for $A^{a\prime}_0$, differentiating it once with respect to u and using (3.17) results in Eq. (3.10) for $\nu = 3$,

$$0 = A^{a\prime\prime}_3 + \frac{f'}{f}A^{a\prime}_3 + \frac{\mathfrak{w}^2}{uf^2}A^a_3 + \frac{\mathfrak{q}\mathfrak{w}}{uf^2}A^a_0 + i\frac{\mathfrak{q}}{uf^2}f^{abc}\frac{\mu^b}{2\pi T}A^c_0 + 2i\frac{\mathfrak{w}}{uf^2}f^{abc}\frac{\mu^b}{2\pi T}A^c_3. \quad (3.19)$$

We will make use of the Eqs. (3.17) and (3.18) which look more concise. These equations of motion for A^a_0 and A^a_3 are coupled in Lorentz and flavor indices. To decouple them with respect to the Lorentz structure, we solve (3.18) for $A^{a\prime}_3$ and insert the result into the differentiated version of (3.17). This gives

$$0 = A^{a\prime\prime\prime}_0 + \frac{(uf)'}{uf}A^{a\prime\prime}_0 + \frac{\mathfrak{w}^2 - f\mathfrak{q}^2}{uf^2}A^{a\prime}_0 + 2i\frac{\mathfrak{w}}{uf^2}f^{abc}\frac{\mu^b}{2\pi T}A^{c\prime}_0. \quad (3.20)$$

The equations for $a = 1, 2$ are still coupled with respect to their gauge structure. The case $a = 3$ was solved in [2]. We will solve (3.20) for $A^{a\prime}_0$ and can obtain $A^{a\prime}_3$ from (3.18). Note that it is sufficient for our purpose to obtain solutions for the derivatives of the fields. These contribute to (2.4), while the functions $A = f(u,\vec{k})A^{\mathrm{bdy}}(\vec{k})$ themselves simply contribute a factor of $f(u,-\vec{k})$ which is 1 at the boundary.

3. Solutions

Generally, we follow the methods developed in [2], since our differential equations are very similar to the ones considered there. Additionally, we need to respect the flavor structure of the gauge fields. The equations for flavor index $a = 3$ resemble the ones analyzed in [2]. However, those for $a = 1, 2$ involve extra terms, which couple these equations. In our case the equations are coupled not only via their Lorentz indices, but also with respect to the flavor indices. We already decoupled the Lorentz structure in the previous section. As shown below, the equations of motion which involve different gauge components will decouple if we consider the variables

$$X_i = A^1_i + iA^2_i, \qquad \tilde{X}_i = A^1_i - iA^2_i. \quad (3.21)$$

Here the A^1_i, A^2_i are the generally complex gauge field components in momentum space. Note that up to $SU(2)$ transformations, the combinations (3.21) are the only ones which decouple the equations of motion for $a = 1, 2$. These combinations are reminiscent of the non-Abelian

$SU(2)$ gauge field in position space,

$$A_i = A_i^a \frac{\sigma^a}{2} = \frac{1}{2}\begin{pmatrix} A_i^3 & A_i^1 - iA_i^2 \\ A_i^1 + iA_i^2 & -A_i^3 \end{pmatrix}. \tag{3.22}$$

The equations of motion for the flavor index $a = 3$ were solved in [2]. To solve the equations of motion for the fields A_i^a with $a = 1, 2$, we rewrite them in terms of X_i and $\tilde{X}_i$. Applying the transformation (3.21) to the equations of motion (3.14) and (3.15) and the $a = 1, 2$ versions of (3.18) and (3.20) leads to

$$0 = X_\alpha'' + \frac{f'}{f} X_\alpha' + \frac{\mathfrak{w}^2 - f\mathfrak{q}^2 \mp 2\mathfrak{m}\mathfrak{w}}{uf^2} X_\alpha, \qquad \alpha = 1, 2, \tag{3.23}$$

$$0 = X_0''' + \frac{(uf)'}{uf} X_0'' + \frac{\mathfrak{w}^2 - f\mathfrak{q}^2 \mp 2\mathfrak{m}\mathfrak{w}}{uf^2} X_0', \tag{3.24}$$

$$0 = (\mathfrak{w} \mp \mathfrak{m}) X_0' + \mathfrak{q} f X_3', \tag{3.25}$$

where the upper signs correspond to X and the lower ones to $\tilde{X}$.

We see that some coefficients of these functions are divergent at the horizon $u = 1$. Such differential equations with singular coefficients are generically solved by an ansatz

$$X_i = (1-u)^\beta F(u), \qquad \tilde{X}_i = (1-u)^{\tilde{\beta}} \tilde{F}(u), \tag{3.26}$$

with regular functions $F(u)$ and $\tilde{F}(u)$. To cancel the singular behavior of the coefficients, we have to find the adequate β and $\tilde{\beta}$, the so-called indices, given by equations known as the indicial equations for β and $\tilde{\beta}$. We eventually get for all X_i and $\tilde{X}_i$

$$\beta = \pm \frac{i\mathfrak{w}}{2}\sqrt{1 - \frac{2\mathfrak{m}}{\mathfrak{w}}}, \qquad \tilde{\beta} = \pm \frac{i\mathfrak{w}}{2}\sqrt{1 + \frac{2\mathfrak{m}}{\mathfrak{w}}}. \tag{3.27}$$

Note that these exponents differ from those of the Abelian super-Maxwell theory [2] by a dependence on $\sqrt{\mathfrak{w}}$ in the limit of small frequencies ($\mathfrak{w} < \mathfrak{m}$). In the limit of vanishing chemical potential $\mathfrak{m} \to 0$, the indices given in [2] are reproduced from (3.27). In order to solve (3.23), (3.24), and (3.25), we wish to introduce a series expansion ansatz in the momentum variables $\mathfrak{w}$ and $\mathfrak{q}$. In fact, the physical motivation behind this expansion is that we aim for thermodynamical quantities which are known from statistical mechanics in the hydrodynamic limit of small four-momentum $\vec{k}$. So the standard choice would be

$$F(u) = F_0 + \mathfrak{w} F_1 + \mathfrak{q}^2 G_1 + \dots. \tag{3.28}$$

On the other hand, we realize that our indices will appear linearly (and quadratically) in the differential equations' coefficients after inserting (3.26) into (3.23), (3.24), and (3.25). The square root in β and $\tilde{\beta}$ mixes different orders of $\mathfrak{w}$. In order to sort coefficients in our series ansatz, we assume $\mathfrak{w} < \mathfrak{m}$ and keep only the leading $\mathfrak{w}$ contributions to β and $\tilde{\beta}$, such that

$$\beta \approx \mp\sqrt{\frac{\mathfrak{w}\mathfrak{m}}{2}}, \qquad \tilde{\beta} \approx \pm i\sqrt{\frac{\mathfrak{w}\mathfrak{m}}{2}}. \tag{3.29}$$

This introduces an additional order $\mathcal{O}(\mathfrak{w}^{1/2})$, which we include in our ansatz (3.28) yielding

$$F(u) = F_0 + \mathfrak{w}^{1/2} F_{1/2} + \mathfrak{w} F_1 + \mathfrak{q}^2 G_1 + \dots, \tag{3.30}$$

and analogously for the tilded quantities. If we had not included $\mathcal{O}(\mathfrak{w}^{1/2})$ the resulting system would be overdetermined. The results we obtain by using the approximations (3.29) and (3.30) have been checked against the numerical solution for exact β with exact $F(u)$. These approximations are useful for fluctuations with $\mathfrak{q}, \mathfrak{w} < 1$ (see Sec. B 4 in Appendix B). Note that by dropping the 1 in (3.27) we also drop the Abelian limit.

Consider the indices (3.27) for positive frequency first. In order to meet the incoming wave boundary condition introduced in Sec. II, we restrict the solution $\tilde{\beta}$ to the negative sign only. For the approximate $\tilde{\beta}$ in (3.29) we therefore choose the lower (negative) sign. This exponent describes a mode that travels into the horizon of the black hole. In case of β we demand the mode to decay towards the horizon, choosing the lower (positive) sign in (3.29) consistently. Note that for negative frequencies $\omega < 0$ the indices β and $\tilde{\beta}$ exchange their roles.

Using (3.29) in (3.26) and inserting the ansatz into the equations of motion, we find equations for each order in $\mathfrak{q}^2$ and $\mathfrak{w}$ separately. After solving the equations of motion for the coefficient functions F_0, $F_{1/2}$, F_1 and G_1, we eventually can assemble the solutions to the equations of motion for X as defined in (3.21),

$$\begin{aligned} X(u) &= (1-u)^\beta F(u) \\ &= (1-u)^\beta (F_0 + \sqrt{\mathfrak{w}} F_{1/2} + \mathfrak{w} F_1 + \mathfrak{q}^2 G_1 + \dots), \end{aligned} \tag{3.31}$$

and a corresponding formula for $\tilde{X}(u)$ from the ansatz (3.26).

Illustrating the method, we now write down the equations of motion order by order for the function X_α. To do so, we use (3.31) with (3.29) in (3.23) with the upper sign for X_α. Then we examine the result order by order in $\mathfrak{w}$ and $\mathfrak{q}^2$,

$$\mathcal{O}(\text{const}):\ 0 = F_0'' + \frac{f'}{f} F_0', \tag{3.32}$$

$$\mathcal{O}(\sqrt{\mathfrak{w}}):\ 0 = F_{1/2}'' + \frac{f'}{f} F_{1/2}' - \frac{\sqrt{2\mathfrak{m}}}{1-u} F_0' - \sqrt{\frac{\mathfrak{m}}{2}} \frac{1}{f} F_0, \tag{3.33}$$

$$\mathcal{O}(\mathfrak{w}):\ 0 = F_1'' + \frac{f'}{f}F_1' - \frac{\sqrt{2\mathfrak{m}}}{1-u}F_{1/2}' - \sqrt{\frac{\mathfrak{m}}{2}}\frac{1}{f}F_{1/2} - \mathfrak{m}\frac{4-u(1+u)^2}{2uf^2}F_0, \tag{3.34}$$

$$\mathcal{O}(\mathfrak{q}^2):\ 0 = G_1'' + \frac{f'}{f}G_1' - \frac{1}{uf}F_0. \tag{3.35}$$

At this point we observe that the differential equations we have to solve for each order are shifted with respect to the solutions found in [2]. The contributions of order $\mathfrak{w}^n$ in [2] now show up in order $\mathfrak{w}^{n/2}$. Their solutions will exhibit factors of order $\mu^{n/2}$.

Solving the system (3.32) to (3.35) of coupled differential equations is straightforward in the way that they can be reduced to several uncoupled first-order ordinary differential equations in the following way. Note that there obviously is a constant solution $F_0 = C$ for the first equation. Inserting it into (3.33) and (3.35) leaves us with ordinary differential equations for $F_{1/2}'$ and G_1', respectively. Using the solutions of F_0 and $F_{1/2}$ in (3.34) gives one more such equation for F_1'.

To fix the boundary values of the solutions just mentioned, we demand the value of $F(u_H = 1)$ to be given by the constant F_0 and therefore choose the other component functions' solutions such that $\lim_{u\to 1} F_{1/2} = 0$, and the same for F_1 and G_1. The remaining integration constant C is determined by taking the boundary limit $u \to 0$ of the explicit solution (3.31), making use of the second boundary condition

$$\lim_{u\to 0} X(u) = X^{\mathrm{bdy}}, \tag{3.36}$$

see Appendix B. Eventually, we end up with all the ingredients needed to construct the gauge field's fluctuations $X(u)$ as in (3.31).

We solve the Eqs. (3.23) with lower sign for $\tilde{X}_\alpha$ and (3.24) for X_0' and its tilded partner in exactly the same way as just outlined, only some coefficients of these differential equations differ. The solution for X_3' is then obtained from (3.25).

All solutions are given explicitly in Appendix B together with all other information needed to construct the functions X_α, $\tilde{X}_\alpha$, X_0', $\tilde{X}_0'$, X_3' and $\tilde{X}_3'$.

IV. ISOSPIN DIFFUSION AND CORRELATION FUNCTIONS

A. Current correlators

In this section we obtain the momentum space correlation functions for the gauge field component combinations X and $\tilde{X}$ defined in Eq. (3.21). Recall that the imaginary part of the retarded correlators essentially gives the thermal spectral functions (see also Sec. II). The following discussion of the correlators' properties is therefore equivalent to a discussion of the corresponding spectral functions.

First note that the on-shell action gets new contributions from the non-Abelian structure,

$$S_{\mathrm{D7}} = -T_7\frac{(2\pi\alpha')^2}{2}2\pi^2R^3T_r2\int\frac{\mathrm{d}^4q}{(2\pi)^4} \times\left[\sqrt{-g}g^{uu}g^{jj'}A_j^{a\prime}(\vec{q})A_{j'}^a(-\vec{q})\Big|_{u_b=0}^{u_h=1} - 4iqf^{abc}\mu^c\int_0^1\mathrm{d}u\sqrt{-g}g^{00}g^{33}A^a_{[3}A^b_{0]}\right], \tag{4.1}$$

where $j, j' = 0, 1, 2, 3$ and the index u denotes the radial AdS direction. Up to the sum over flavor indices, the first term in the bracket is similar to the Abelian super-Maxwell action of [2]. The second term is a new contribution depending on the isospin chemical potential. It is a contact term which we will neglect. The correlation functions however get a structure that is different from the Abelian case. This is due to the appearance of the chemical potential in the equations of motion and their solutions. Writing (4.1) as a function of X and $\tilde{X}$ results in

$$S_{\mathrm{D7}} = -T_7\frac{(2\pi\alpha')^2}{2}2\pi^2R^3T_r2\int\frac{\mathrm{d}^4q}{(2\pi)^4}\Big\{\sqrt{-g}g^{uu}g^{jj'} \times\left[\frac{1}{2}(X_j'\tilde{X}_{j'} + \tilde{X}_j'X_{j'}) + A_j^{3\prime}A_{j'}^3\right]\Big|_{u_b=0}^{u_h=1} - 4q\mu\int_0^1\mathrm{d}u\sqrt{-g}g^{00}g^{33}(X_{[0}\tilde{X}_{3]} + \tilde{X}_{[3}X_{0]})\Big\}. \tag{4.2}$$

In order to find the current correlators, we apply the method outlined in Sec. II to (4.2), with the solutions for the fields given in Appendix B. As an example, we derive the correlators $G_{0\tilde{0}} = \langle J_0(\vec{q})\tilde{J}_0(-\vec{q})\rangle$ and $G_{\tilde{0}0} = \langle\tilde{J}_0(\vec{q})J_0(-\vec{q})\rangle$ of the flavor current time components J_0 and $\tilde{J}_0$, coupling to the bulk fields X_0 and $\tilde{X}_0$, respectively. Correlation functions of all other components are derived analogously. For the notation see Appendix A.

1. Green functions: Calculation

First, we extract the factor $B(u)$ of (2.2),

$$B(u) = -T_7\frac{(2\pi\alpha')^2}{2}2\pi^2R^3T_r\sqrt{-g}g^{uu}g^{00}. \tag{4.3}$$

The second step, finding the solutions to the mode equations of motion, has already been performed in Sec. III D 3. In the example at hand we need the solutions X_0 and $\tilde{X}_0$. From (3.31) and from Appendix B we obtain

$$X_0' = -(1-u)^{\sqrt{\mathfrak{w}\mathfrak{m}/2}} \frac{\mathfrak{q}^2 \tilde{X}_0^{\mathrm{bdy}} + \mathfrak{w}\mathfrak{q}\tilde{X}_3^{\mathrm{bdy}}}{\sqrt{2\mathfrak{m}\mathfrak{w}} + \mathfrak{w}\mathfrak{m}\ln 2 + \mathfrak{q}^2} \times \Bigg[1 - \mathfrak{w}^{1/2}\sqrt{\frac{\mathfrak{m}}{2}}\ln\Big(\frac{2u^2}{u+1}\Big) - \mathfrak{w}\frac{\mathfrak{m}}{12}\Big(\pi^2 + 3\ln^2 2 + 3\ln^2(1+u) + 6\ln 2 \ln\Big(\frac{u^2}{1+u}\Big) + 12\mathrm{Li}_2(1-u) + 12\mathrm{Li}_2(-u) - 12\mathrm{Li}_2\Big(\frac{1-u}{2}\Big)\Big) + \mathfrak{q}^2\ln\Big(\frac{u+1}{2u}\Big)\Bigg], \tag{4.4}$$

$$\tilde{X}_0' = -(1-u)^{-i\sqrt{\mathfrak{w}\mathfrak{m}/2}} \frac{\mathfrak{q}^2 X_0^{\mathrm{bdy}} + \mathfrak{w}\mathfrak{q}X_3^{\mathrm{bdy}}}{i\sqrt{2\mathfrak{m}\mathfrak{w}} + \mathfrak{w}\mathfrak{m}\ln 2 - \mathfrak{q}^2} \times \Bigg[1 + \mathfrak{w}^{1/2} i\sqrt{\frac{\mathfrak{m}}{2}}\ln\Big(\frac{2u^2}{u+1}\Big) + \mathfrak{w}\frac{\mathfrak{m}}{12}\Big(\pi^2 + 3\ln^2 2 + 3\ln^2(1+u) + 6\ln 2 \ln\Big(\frac{u^2}{1+u}\Big) + 12\mathrm{Li}_2(1-u) + 12\mathrm{Li}_2(-u) - 12\mathrm{Li}_2\Big(\frac{1-u}{2}\Big)\Big) + \mathfrak{q}^2\ln\Big(\frac{u+1}{2u}\Big)\Bigg]. \tag{4.5}$$

Note that we need the derivatives to apply (2.4).

Now we perform the third step and insert (4.3), (4.4), and (4.5) into (2.4). Our solutions X_0 and $\tilde{X}_0$ replace the solution $f(u,\vec{k})$ and $f(u,-\vec{k})$ in (2.4). The resulting expression is evaluated at $u_b = 0$, which comes from the lower limit of the u-integral in the on-shell action (4.2). At small $u = \epsilon \to 0$, (4.4) and (4.5) give

$$\lim_{u\to 0} X_0' = -\frac{\mathfrak{q}^2\tilde{X}_0^{\mathrm{bdy}} + \mathfrak{w}\mathfrak{q}\tilde{X}_3^{\mathrm{bdy}}}{\sqrt{2\mathfrak{m}\mathfrak{w}} + \mathfrak{w}\mathfrak{m}\ln 2 + \mathfrak{q}^2} - \lim_{\epsilon\to 0}(\mathfrak{q}^2\tilde{X}_0^{\mathrm{bdy}} + \mathfrak{w}\mathfrak{q}\tilde{X}_3^{\mathrm{bdy}})\ln\epsilon, \tag{4.6}$$

$$\lim_{u\to 0} \tilde{X}_0' = -\frac{\mathfrak{q}^2 X_0^{\mathrm{bdy}} + \mathfrak{w}\mathfrak{q}X_3^{\mathrm{bdy}}}{i\sqrt{2\mathfrak{m}\mathfrak{w}} + \mathfrak{w}\mathfrak{m}\ln 2 - \mathfrak{q}^2} + \lim_{\epsilon\to 0}(\mathfrak{q}^2 X_0^{\mathrm{bdy}} + \mathfrak{w}\mathfrak{q}X_3^{\mathrm{bdy}})\ln\epsilon. \tag{4.7}$$

In the next-to-leading order of (4.6) and (4.7) there appear singularities, just like in the Abelian super-Maxwell calculation [Ref. [2], Eq. (5.15)]. However, in the hydrodynamic limit, we consider only the finite leading order.

2. Green functions: Results

Putting everything together, for the two Green functions for the field components X_0, $\tilde{X}_0$ given in (3.21) by

$$X_0 = A_0^1 + iA_0^2, \qquad \tilde{X}_0 = A_0^1 - iA_0^2,$$

we obtain

$$G_{0\tilde{0}} = \frac{N_c T}{8\pi} \frac{2\pi T\mathfrak{q}^2}{-\sqrt{2\mathfrak{m}\mathfrak{w}} - \mathfrak{q}^2 - \mathfrak{w}\mathfrak{m}\ln 2}, \tag{4.8}$$

$$G_{\tilde{0}0} = \frac{N_c T}{8\pi} \frac{2\pi T\mathfrak{q}^2}{i\sqrt{2\mathfrak{m}\mathfrak{w}} - \mathfrak{q}^2 + \mathfrak{w}\mathfrak{m}\ln 2}. \tag{4.9}$$

These are the Green functions for the time components in Minkowski space, perpendicular to the chemical potential in flavor space. All Green functions are obtained considering hydrodynamic approximations in $\mathcal{O}(\mathfrak{w}^{1/2}, \mathfrak{w}, \mathfrak{q}^2)$, neglecting mixed and higher orders $\mathcal{O}(\mathfrak{w}^{3/2}, \mathfrak{w}^{1/2}\mathfrak{q}^2, \mathfrak{q}^4)$.

The prefactor in (4.8) and (4.9) is obtained using T_7 as in (3.7), and carefully inserting all metric factors, together with the standard AdS/CFT relation $R^4 = 4\pi g_s N_c \alpha'^2$. As in other settings with flavor [26], we concordantly get an overall factor of N_c, and not N_c^2, for all correlators. Contrary to those approaches, we do not get a factor of N_f when summing over the different flavors. This is due to the fact that in our setup, the individual flavors yield distinct contributions. Most striking is the nontrivial dependence on the (dimensionless) chemical potential $\mathfrak{m}$ in both correlators. Note also the distinct structures in the denominators. The first one (4.8) has no explicit relative factor of i between the terms in the denominator. In the second correlator (4.9) there is an explicit factor of i. The correlator (4.9) has a complex denominator structure in $\sqrt{\omega}$ for $\omega > 0$, but is entirely real for $\omega < 0$. On the other hand, (4.8) is real for $\omega > 0$ but develops a diffusion structure for $\omega < 0$. So the correlators $G_{0\tilde{0}}$ and $G_{\tilde{0}0}$ essentially exchange their roles as ω changes sign (see also Fig. 1). We find a similar behavior for all correlators $G_{j\tilde{l}}$ and $G_{\tilde{j}l}$ with $j, l = 0, 1, 2, 3$. This behavior is a consequence of the insertion of $\mathcal{O}(\mathfrak{w}^{1/2})$ in the hydrodynamic expansion (3.30).

We assume $\mathfrak{m}$ to be small enough in order to neglect the denominator term of order $\mathcal{O}(\mathfrak{w}\mathfrak{m}) \ll \mathcal{O}(\sqrt{\mathfrak{w}\mathfrak{m}}, \mathfrak{q}^2)$. Moreover, using the definitions of $\mathfrak{w}$, $\mathfrak{q}$ and $\mathfrak{m}$ from (3.13) we may write (4.8) and (4.9) as

$$G_{0\tilde{0}} = -\frac{N_c T}{8\pi\sqrt{2\mu}} \frac{q^2\sqrt{\omega}}{\omega + q^2 D(\omega)}, \tag{4.10}$$

$$G_{\tilde{0}0} = \frac{N_c T}{8\pi\sqrt{2\mu}} \frac{q^2\sqrt{\omega}}{i\omega - q^2 D(\omega)}, \tag{4.11}$$

where the frequency-dependent diffusion coefficient $D(\omega)$ is given by

$$D(\omega) = \sqrt{\frac{\omega}{2\mu}} \frac{1}{2\pi T}. \tag{4.12}$$

We observe that this coefficient also depends on the inverse square root of the chemical potential μ. Its physical interpretation is discussed below in Sec. IV B.

In the same way we derive the other correlation functions

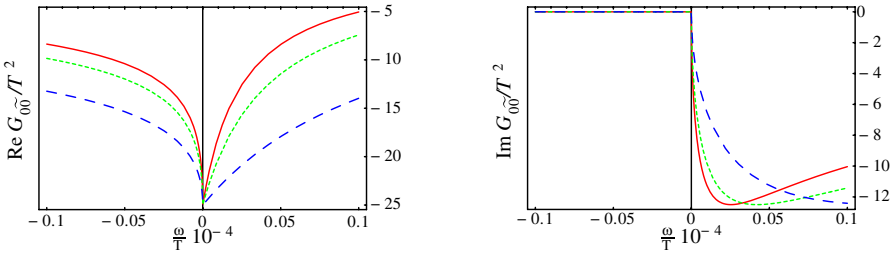

FIG. 1 (color online). Real (left plot) and imaginary part (right plot) of the correlator $G_{0\tilde{0}}$ as a function of frequency ω/T at different chemical potential values $\mu/T = 0.5$ (solid line), $\mu/T = 0.3$ (short-dashed line) and $\mu/T = 0.1$ (long-dashed line). The corresponding plots for the correlator $G_{\tilde{0}0}$ would look like the mirror image of the ones given. The real part would be reflected about the vertical axis at $\omega = 0$, the imaginary part would be reflected about the origin. All dimensionful quantities are given in units of temperature. The numerical values used for the parameters are $q/T = 0.1$, $N_c = 100$.

$$G_{3\tilde{3}} = -\frac{N_c T}{8\pi\sqrt{2\mu}}\frac{\omega^{3/2}(\omega-\mu)}{\tilde{Q}(\omega,q)}, \qquad G_{\tilde{3}3} = \frac{N_c T}{8\pi\sqrt{2\mu}}\frac{\omega^{3/2}(\omega+\mu)}{Q(\omega,q)}, \tag{4.13}$$

$$G_{0\tilde{3}} = -\frac{N_c T}{8\pi\sqrt{2\mu}}\frac{\sqrt{\omega}q(\omega-\mu)}{\tilde{Q}(\omega,q)}, \qquad G_{\tilde{0}3} = \frac{N_c T}{8\pi\sqrt{2\mu}}\frac{\sqrt{\omega}q(\omega+\mu)}{Q(\omega,q)}, \tag{4.14}$$

$$G_{3\tilde{0}} = -\frac{N_c T}{8\pi\sqrt{2\mu}}\frac{\omega^{3/2}q}{\tilde{Q}(\omega,q)}, \qquad G_{\tilde{3}0} = \frac{N_c T}{8\pi\sqrt{2\mu}}\frac{\omega^{3/2}q}{Q(\omega,q)}, \tag{4.15}$$

with the short-hand notation

$$Q(\omega,q) = i\omega - q^2 D(\omega), \qquad \tilde{Q}(\omega,q) = \omega + q^2 D(\omega). \tag{4.16}$$

Note that most of these functions are proportional to powers of q and therefore vanish in the limit of vanishing spatial momentum $q \to 0$. Only the 33-combinations from (4.13) survive this limit. In contrast to the Abelian super-Maxwell correlators [2] given in Appendix C, it stands out that our results (4.10), (4.11), (4.13), and (4.15) have a new zero at $\omega = \mu$ or $-\mu$. Nevertheless bear in mind that we took the limit $\omega < \mu$ in order to obtain our solutions. Therefore the apparent zeros at $\pm\mu$ lie outside of the range considered. Compared to the Abelian case there is an additional factor of $\sqrt{\omega}$. The dependence on temperature remains linear.

In the remaining X-correlators we do not find any pole structure to order $\sqrt{\omega}$, subtracting an $\mathcal{O}(q^2)$ contribution as in [2],

$$G_{1\tilde{1}} = G_{2\tilde{2}} = \frac{\sqrt{2}N_c T}{8\pi}\sqrt{\mu\omega}, \tag{4.17}$$

$$G_{\tilde{1}1} = G_{\tilde{2}2} = -\frac{i\sqrt{2}N_c T}{8\pi}\sqrt{\mu\omega}. \tag{4.18}$$

As seen from (4.17), $G_{\alpha\tilde{\alpha}}$ (with $\alpha = 1, 2$) are real for negative ω and imaginary for positive ω. The opposite is true for $G_{\tilde{\alpha}\alpha}$, as is obvious from the relative factor of i.

The correlators of components, pointing along the isospin potential in flavor space ($a = 3$), are found to be

$$G_{A_0^3 A_0^3} = \frac{N_c T}{4\pi}\frac{q^2}{i\omega - D_0 q^2}, \qquad G_{A_0^3 A_3^3} = G_{A_3^3 A_0^3} = \frac{N_c T}{4\pi}\frac{\omega q}{i\omega - D_0 q^2}, \tag{4.19}$$

$$G_{A_1^3 A_1^3} = G_{A_2^3 A_2^3} = -\frac{N_c T i\omega}{4\pi}, \qquad G_{A_3^3 A_3^3} = \frac{N_c T}{4\pi}\frac{\omega^2}{i\omega - D_0 q^2}, \tag{4.20}$$

with the diffusion constant $D_0 = 1/(2\pi T)$. Note that these latter correlators have the same structure but differ by a factor $4/N_c$ from those found in the Abelian super-Maxwell case [2] [see also (C1) and (C2)]. In particular the correlators in Eq. (4.19) do not depend on the chemical potential.

To analyze the novel structures appearing in the other correlators, we explore their real and imaginary parts as well as the interrelations among them,

$$\mathrm{Re}\, G_{0\tilde{0}}(\omega \geq 0) = -\mathrm{Re}\, G_{\tilde{0}0}(\omega < 0) = -\frac{N_c T}{8\pi}\frac{q^2}{\sqrt{2\mu|\omega|} + q^2/(2\pi T)}, \tag{4.21}$$

$$\mathrm{Re}\; G_{0\tilde{0}}(\omega < 0) = -\mathrm{Re}\, G_{\tilde{0}0}(\omega \geq 0) = -\frac{N_c T}{16\pi^2}\frac{q^4}{2\mu|\omega| + q^4/(2\pi T)^2}, \tag{4.22}$$

$$\mathrm{Im}\, G_{0\tilde{0}}(\omega < 0) = -\mathrm{Im}\, G_{\tilde{0}0}(\omega \geq 0) = -\frac{N_c T}{8\pi} \frac{q^2\sqrt{2\mu|\omega|}}{2\mu|\omega| + q^4/(2\pi T)^2}, \quad (4.23)$$

and

$$\mathrm{Im}\, G_{0\tilde{0}}(\omega \geq 0) = 0, \qquad \mathrm{Im}\, G_{\tilde{0}0}(\omega < 0) = 0. \quad (4.24)$$

Now we see why, as discussed below (4.11), $G_{0\tilde{0}}$ and $G_{\tilde{0}0}$ exchange their roles when crossing the origin at $\omega = 0$. This is due to the fact that the real parts of all $G_{j\tilde{l}}$ and $G_{\tilde{j}l}$ are mirror images of each other by reflection about the vertical axis at $\omega = 0$. In contrast, the imaginary parts are inverted into each other at the origin. Figure 1 shows the real and imaginary parts of correlators $G_{0\tilde{0}}$ and $G_{\tilde{0}0}$. The different curves correspond to distinct values of the chemical potential μ. The real part shows a deformed resonance behavior. The imaginary part has a deformed interference shape with vanishing value for negative frequencies. All curves are continuous and finite at $\omega = 0$. However due to the square-root dependence, they are not differentiable at the origin. Parts of the correlator which are real for positive ω are shifted into the imaginary part by the change of sign when crossing $\omega = 0$, and vice versa.

To obtain physically meaningful correlators, we follow a procedure which generalizes the Abelian approach of [6]. In the Abelian case, gauge-invariant components of the field strength tensor, such as $E_\alpha = \omega A_\alpha$, are considered as physical variables. This procedure cannot be transferred directly to the non-Abelian case. Instead, we consider the nonlocal part of the gauge-invariant $\mathrm{tr}F^2$ which contributes to the on-shell action (4.1). In this action, the contribution involving the non-Abelian structure constant—as well as μ—is a local contact term. The nonlocal contribution however generates the Green function combination

$$G_{A_i^1 A_j^1} + G_{A_i^2 A_j^2} + G_{A_i^3 A_j^3}. \quad (4.25)$$

We take this sum as our physical Green function. This choice is supported further by the fact that it may be written in terms of the linear combinations (3.21) which decouple the equations of motion. For example, for the time component, written in the variables X_0, $\tilde{X}_0$ given by (3.21), the combination (4.25) reads [compare to (4.2)]

$$G_{0\tilde{0}} + G_{\tilde{0}0} + G_{A_0^3 A_0^3}. \quad (4.26)$$

The contribution from $G_{A_0^3 A_0^3}$ is of order $\mathcal{O}(\mu^0)$, while the combination for the first two flavor directions, $G_{0\tilde{0}} + G_{\tilde{0}0}$, is of order $\mathcal{O}(\mu)$.

We proceed by discussing the physical behavior of the Green function combinations introduced above. $G_{A_0^3 A_0^3}$ is plotted in Fig. 2 on the right. Its frequency dependence is of the same form as in the Abelian correlator obtained in [2], as can be seen from (C1). Since we are interested in effects of order $\mathcal{O}(\mu)$, we drop the third flavor direction $a = 3$ from the sum (4.26) in the following. It is reassuring to observe that the flavor directions $a = 1, 2$, which are orthogonal to the chemical potential, combine to give a correlator spectrum qualitatively similar to the one found in [2] for the Abelian super-Maxwell action (see Fig. 2). However, we discover intriguing new effects such as the highly increased steepness of the curves near the origin due to the square-root dependence and a kink at the origin.

We observe a narrowing of the inverse resonance peak compared to the form found for the Abelian super-Maxwell action (and also compared to the form of our $G_{A_0^3 A_0^3}$, as is seen from comparing the left with the right plot in Fig. 2). At the origin the real and imaginary part are finite and continuous, but they are not continuously differentiable. However, the imaginary part of $G_{A_0^3 A_0^3}$ has finite steepness at the origin. The real part though has vanishing derivative at $\omega = 0$. Note that the imaginary part of flavor directions $a = 1, 2$ on the left plot in Fig. 2 never drops below the real part. In the third flavor direction, as well as in the Abelian solution, such a drop occurs on the positive ω-axis.

The correlators $G_{3\tilde{3}}$, $G_{\tilde{3}3}$, $G_{0\tilde{3}}$ and $G_{\tilde{0}3}$ have the same interrelations between their respective real and imaginary parts as $G_{0\tilde{0}}$ and $G_{\tilde{0}0}$. Nevertheless, their dependence on the frequency and momentum is different, as can be seen from (4.13) to (4.15). A list of the 33-direction Green functions

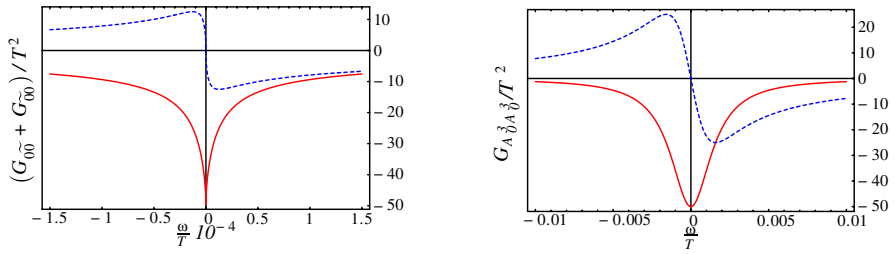

FIG. 2 (color online). In the left plot the sum of both correlators in 00-directions is split into its imaginary (dashed line) and real (solid line) part and plotted against frequency. For comparison the right plot shows the corresponding real and imaginary parts for the $G_{A_0^3 A_0^3}$. It is qualitatively similar to the Abelian correlator in $i = 0$ Lorentz direction computed from the super-Maxwell action in [2]. Note the different frequency scales in the two plots. The curves in $a = 1$, 2-directions are much narrower due to their square-root dependence on ω. Furthermore they have a much larger maximum amplitude. All dimensionful quantities are given in units of temperature. The numerical values used for the parameters are, as in Fig. 1, $q/T = 0.1$, $N_c = 100$ and only in the left plot $\mu/T = 0.2$.

split into real and imaginary parts can be found in Appendix D.

Thermal spectral functions in different directions are compared graphically in Appendix E.

B. Isospin diffusion

The attenuated poles in hydrodynamic correlation functions have specific meanings (for exemplary discussions of this in the AdS/CFT setup see e.g. [7,50]). In our case we observe an attenuated pole in the sum $G_{0\tilde{0}} + G_{\tilde{0}0}$ at $\omega = 0$. As can be seen from the plots in Fig. 2, our pole lies at $\mathrm{Re}\omega = 0$. This structure appears in hydrodynamics as the signature of a diffusion pole located at purely imaginary ω. Its location on the imaginary ω-axis is given by the zeros of the denominators of our correlators as [neglecting $\mathcal{O}(\omega, q^4)$]

$$\sqrt{\omega} = -i\frac{q^2}{2\pi T\sqrt{2\mu}}. \tag{4.27}$$

Squaring both sides of (4.27) we see that this effect is of order $\mathcal{O}(q^4)$. On the other hand, looking for poles in the correlator involving the third flavor direction $G_{A_0^3 A_0^3}$, we obtain dominant contributions of order $\mathcal{O}(q^2)$ and $\mathcal{O}(\mu^0)$ [neglecting $\mathcal{O}(\omega^2, q^2)$]

$$\omega = -i\frac{q^2}{2\pi T}. \tag{4.28}$$

This diffusion pole is reminiscent of the result of the Abelian result of [2] given in Appendix (C). As discussed in Sec. IVA, we consider gauge-invariant combinations $G_{0\tilde{0}} + G_{\tilde{0}0} + G_{A_0^3 A_0^3}$. In order to inspect the non-Abelian effects of order $\mathcal{O}(\mu)$ showing up in the first two correlators in this sum, we again drop the third flavor direction which is of order $\mathcal{O}(\mu^0)$.

Motivated by the diffusion pole behavior of our correlators in flavor directions $a = 1, 2$ corresponding to the combinations X, $\tilde{X}$ [see (4.27)], we wish to regain the structure of the diffusion equation given in (2.9), which in our coordinates [$k = (\omega, 0, 0, q)$] reads

$$i\omega J_0 = D(\omega) q^2 J_0. \tag{4.29}$$

Our goal is to rewrite (4.27) such that a term $\mathcal{O}(\omega)$ and one term in order $\mathcal{O}(q^2)$ appears. Furthermore there should be a relative factor of $-i$ between these two terms. The obvious manipulation to meet these requirements is to multiply (4.27) by $\sqrt{\omega}$ in order to get

$$\omega = -iq^2\frac{\sqrt{\omega}}{2\pi T\sqrt{2\mu}}. \tag{4.30}$$

Comparing the gravity result (4.30) with the hydrodynamic Eq. (4.29), we obtain the frequency-dependent diffusion coefficient

$$D(\omega) = \sqrt{\frac{\omega}{2\mu}}\frac{1}{2\pi T}. \tag{4.31}$$

Our argument is thus summarized as follows: Given the isospin chemical potential as in (1.1) and (3.5), J_0 from (2.9) is the isospin charge density in (4.29). According to (4.29), the coefficient (4.31) describes the diffusive response of the quark-gluon plasma to a gradient in the isospin charge distribution. For this reason we interpret $D(\omega)$ as the isospin diffusion coefficient.

Near the pole, the strongly coupled plasma behaves analogously to a diffractive medium with anomalous dispersion in optics. In the presence of the isospin chemical potential, the propagation of non-Abelian gauge fields in the black hole background depends on the square root of the frequency. In the dual gauge theory, this corresponds to a nonexponential decay of isospin fluctuations with time.

The square-root dependence of our diffusion coefficient is valid for small frequencies. As long as $\omega/T < 1/4$, the square root is larger than its argument, and at $\omega/T = 1/4$, the difference to a linear dependence on frequency is maximal. Therefore in the regime of small frequencies $\omega/T < 1/4$, which is accessible to our approximation, diffusion of modes close to $1/4$ is enhanced compared to modes with frequencies close to zero.

V. CONCLUSION

In this paper we have considered a relatively simple gauge/gravity dual model for a finite temperature field theory, consisting of an isospin chemical potential μ obtained from a time component VEV for the $SU(2)$ gauge field on two coincident brane probes. We have considered the D7-brane embedding corresponding to vanishing quark mass, for which μ is a constant, independent, in particular, of the radial holographic coordinate. The main result of this paper is that this model, despite its simplicity, leads to a hydrodynamical behavior of the dual field theory which goes beyond linear response theory. We find, in particular, a frequency-dependent diffusion coefficient with a non-analytical behavior. Frequency-dependent diffusion is a well-known phenomenon in condensed matter physics. Here it originates simply from the fact that due to the non-Abelian structure of the gauge field on the brane probe, the chemical potential replaces a time derivative in the action and in the equations of motion from which the Green functions are obtained.

Of course the calculation presented has some limitations as far as the approximations made are concerned. This applies, in particular, to the approximation (3.29) of the so-called indices in the ansatz for solving the equations of motion. Here we have dropped the constant present under the square root and used an expression proportional to the square root of the frequency. This allows for a closed solution without having to use numerics. However, using this approximation, we have dropped the Abelian limit.

This leads ultimately to the square-root dependence of the diffusion coefficient on the frequency. This dependence is unphysical for $\omega \to 0$, since the diffusion coefficient is expected to be nonzero for zero frequency. We expect physical behavior to be restored if the Abelian limit is included in the calculation. To avoid the approximation described, this requires a numerical approach. A suitable solution method for all momenta and all frequencies has been presented in [7] and in [49]. We are going to study the application of this method to the model presented here in the future.

ACKNOWLEDGMENTS

We are grateful to R. Apreda, G. Policastro, C. Sieg, A. Starinets and L. Yaffe for useful discussions and correspondence.

APPENDIX A: NOTATION

The five-dimensional AdS-Schwarzschild black hole space in which we work is endowed with a metric of signature $(-, +, +, +, +)$, as given explicitly in (3.3). We make use of the Einstein notation to indicate sums over Lorentz indices, and additionally simply sum over non-Lorentz indices, such as gauge group indices, whenever they occur twice in a term.

To distinguish between vectors in different dimensions of the AdS space, we use bold symbols like $\boldsymbol{q}$ for vectors in the *three spatial dimensions* which do not live along the radial AdS coordinate. *Four-vectors* which do not have components along the radial AdS coordinates are denoted by symbols with an arrow on top, as $\vec{q}$.

The Green functions $G = \langle J\hat{J}\rangle$ considered give correlations between currents J and $\hat{J}$. These currents couple to fields A and $\hat{A}$, respectively. In our notation we use symbols such as $G_{A_k^a A_l^b}$ to denote correlators of currents coupling to fields A_k^a and A_l^b, with flavor indices a, b and Lorentz indices k, $l = 0, 1, 2, 3$. For the gauge field combinations X_k and $\tilde{X}_l$ given in (3.21), we obtain Green functions $G_{k\tilde{l}}$ denoting correlators of the corresponding currents.

APPENDIX B: SOLUTIONS TO EQUATIONS OF MOTION

Here we explicitly write down the component functions used to construct the solutions to the equations of motion for the gauge field fluctuations up to order $\mathfrak{w}$ and $\mathfrak{q}^2$. The functions themselves are then composed as in (3.31).

The solutions for the components with flavor index $a = 3$ were obtained in [2].

1. Solutions for X_α, $\tilde{X}_\alpha$ and A^3_α

The function $X_\alpha(u)$ solves (3.23) with the upper sign and is constructed as in (3.31) from the following component functions,

$$\beta = \sqrt{\frac{\mathfrak{w}\mathfrak{m}}{2}} + \mathcal{O}(\omega), \tag{B1}$$

$$F_0 = C, \tag{B2}$$

$$F_{1/2} = -C\sqrt{\frac{\mathfrak{m}}{2}}\ln\frac{1+u}{2}, \tag{B3}$$

$$\begin{aligned} F_1 = -C\frac{\mathfrak{m}}{12}\Big[& \pi^2 - 9\ln^2 2 + 3\ln(1-u)(\ln 16 - 4\ln(1+u)) \\ & + 3\ln(1+u)(\ln(4(1+u)) - 4\ln u) \\ & - 12\Big(\mathrm{Li}_2(1-u) + \mathrm{Li}_2(-u) + \mathrm{Li}_2\Big(\frac{1+u}{2}\Big)\Big)\Big], \end{aligned} \tag{B4}$$

$$G_1 = \frac{C}{2}\Big[\frac{\pi^2}{12} + \ln u \ln(1+u) + \mathrm{Li}_2(1-u) + \mathrm{Li}_2(-u)\Big], \tag{B5}$$

where the constant C can be expressed in terms of the field's boundary value $X^{\mathrm{bdy}} = \lim_{u\to 0} X(u, k)$,

$$\begin{aligned} C = X^{\mathrm{bdy}}\Big(1 + \sqrt{\frac{\mathfrak{m}\mathfrak{w}}{2}}\ln 2 + \mathfrak{m}\mathfrak{w}\Big(\frac{\pi^2}{6} + \frac{\ln^2 2}{4}\Big) + \frac{\pi^2}{8}\mathfrak{q}^2 \\ + \mathcal{O}(\mathfrak{w}^{3/2}, \mathfrak{q}^4)\Big)^{-1}. \end{aligned} \tag{B6}$$

The solutions of the equations of motion (3.23) with lower sign for the functions $\tilde{X}_\alpha(u)$ are given by

$$\tilde{\beta} = -i\sqrt{\frac{\mathfrak{w}\mathfrak{m}}{2}} + \mathcal{O}(\omega), \tag{B7}$$

$$\tilde{F}_0 = \tilde{C}, \tag{B8}$$

$$\tilde{F}_{1/2} = i\tilde{C}\sqrt{\frac{\mathfrak{m}}{2}}\ln\frac{1+u}{2}, \tag{B9}$$

$$\begin{aligned} \tilde{F}_1 = \tilde{C}\frac{\mathfrak{m}}{12}\Big[& \pi^2 - 9\ln^2 2 + 3\ln(1-u)(\ln 16 - 4\ln(1+u)) \\ & + 3\ln(1+u)(\ln(4(1+u)) - 4\ln u) \\ & - 12\Big(\mathrm{Li}_2(1-u) + \mathrm{Li}_2(-u) + \mathrm{Li}_2\Big(\frac{1+u}{2}\Big)\Big)\Big], \end{aligned} \tag{B10}$$

$$\tilde{G}_1 = \frac{\tilde{C}}{2}\Big[\frac{\pi^2}{12} + \ln u \ln(1+u) + \mathrm{Li}_2(1-u) + \mathrm{Li}_2(-u)\Big], \tag{B11}$$

with $\tilde{C}$ given by

$$\tilde{C} = \tilde{X}^{\rm bdy}\Big(1 - i\sqrt{\frac{\mathfrak{m}\mathfrak{w}}{2}}\ln 2 - \mathfrak{m}\mathfrak{w}\Big(\frac{\pi^2}{6} + \frac{\ln^2 2}{4}\Big) + \frac{\pi^2}{8}\mathfrak{q}^2 + \mathcal{O}(\mathfrak{w}^{3/2}, \mathfrak{q}^4)\Big)^{-1}, \tag{B12}$$

so that $\lim_{u\to 0}\tilde{X}(u,k) = \tilde{X}^{\rm bdy}$.

The solution for A^3_α solves (3.16) up to order $\mathfrak{w}$ and $\mathfrak{q}^2$ with boundary value $(A^3_\alpha)^{\rm bdy}$. It is

$$A^3_\alpha = \frac{8(A^3_\alpha)^{\rm bdy}(1-u)^{-(i\mathfrak{w}/2)}}{8 - 4i\mathfrak{w}\ln 2 + \pi^2\mathfrak{q}^2}\Big[1 + i\frac{\mathfrak{w}}{2}\ln\frac{1+u}{2} + \frac{\mathfrak{q}^2}{2} \times \Big(\frac{\pi^2}{12} + \ln u \ln(1+u) + \mathrm{Li}_2(1-u) + \mathrm{Li}_2(-u)\Big)\Big]. \tag{B13}$$

2. Solutions for X_0', $\tilde{X}_0'$ and $A_0^{3\prime}$

Here we state the solutions to (3.20). This formula describes three equations, differing in the choice of $a = 1, 2, 3$. The cases $a = 1, 2$ give coupled equations which are decoupled by transformation from $A_0^{1,2}$ to X_0 and $\tilde{X}_0$. The choice $a = 3$ gives a single equation.

The function X_0' is the solution to (3.24) with upper sign. We specify the component functions as

$$\beta = \sqrt{\frac{\mathfrak{w}\mathfrak{m}}{2}} + \mathcal{O}(\omega), \tag{B14}$$

$$F_0 = C, \tag{B15}$$

$$F_{1/2} = -C\sqrt{\frac{\mathfrak{m}}{2}}\ln\frac{2u^2}{1+u}, \tag{B16}$$

$$F_1 = -C\frac{\mathfrak{m}}{12}\Big[\pi^2 + 3\ln^2 2 + 3\ln^2(1+u) + 6\ln 2\ln\frac{u^2}{1+u} + 12\Big(\mathrm{Li}_2(1-u) + \mathrm{Li}_2(-u) - \mathrm{Li}_2\Big(\frac{1-u}{2}\Big)\Big)\Big], \tag{B17}$$

$$G_1 = C\ln\frac{1+u}{2u}, \tag{B18}$$

where the constant C can be expressed in terms of the field's boundary value $X^{\rm bdy} = \lim_{u\to 0}X(u,k)$,

$$C = -\frac{\mathfrak{q}^2 X_0^{\rm bdy} + \mathfrak{w}\mathfrak{q}X_3^{\rm bdy}}{\sqrt{2\mathfrak{m}\mathfrak{w}} + \mathfrak{m}\mathfrak{w}\ln 2 + \mathfrak{q}^2}. \tag{B19}$$

To get the function $\tilde{X}_0'$, we solve (3.24) with the lower sign and obtain

$$\tilde{\beta} = -i\sqrt{\frac{\mathfrak{w}\mathfrak{m}}{2}} + \mathcal{O}(\omega), \tag{B20}$$

$$\tilde{F}_0 = \tilde{C}, \tag{B21}$$

$$\tilde{F}_{1/2} = i\tilde{C}\sqrt{\frac{\mathfrak{m}}{2}}\ln\frac{2u^2}{1+u}, \tag{B22}$$

$$\tilde{F}_1 = \tilde{C}\frac{\mathfrak{m}}{12}\Big[\pi^2 + 3\ln^2 2 + 3\ln^2(1+u) + 6\ln 2\ln\frac{u^2}{1+u} + 12\Big(\mathrm{Li}_2(1-u) + \mathrm{Li}_2(-u) - \mathrm{Li}_2\Big(\frac{1-u}{2}\Big)\Big)\Big], \tag{B23}$$

$$\tilde{G}_1 = \tilde{C}\ln\frac{1+u}{2u}, \tag{B24}$$

where the constant $\tilde{C}$ can be expressed it in terms of the field's boundary value $\tilde{X}^{\rm bdy} = \lim_{u\to 0}\tilde{X}(u,k)$,

$$\tilde{C} = \frac{\mathfrak{q}^2\tilde{X}_0^{\rm bdy} + \mathfrak{w}\mathfrak{q}\tilde{X}_3^{\rm bdy}}{i\sqrt{2\mathfrak{m}\mathfrak{w}} + \mathfrak{m}\mathfrak{w}\ln 2 - \mathfrak{q}^2}. \tag{B25}$$

The solution for (3.20) with $a = 3$ is the function $A_0^{3\prime}$, given by

$$A_0^{3\prime} = (1-u)^{-(i\mathfrak{w}/2)}\frac{\mathfrak{q}^2 A_0^{\rm bdy} + \mathfrak{w}\mathfrak{q}A_3^{\rm bdy}}{i\mathfrak{w} - \mathfrak{q}^2}\Big(1 + \frac{i\mathfrak{w}}{2}\ln\frac{2u^2}{1+u} + \mathfrak{q}^2\ln\frac{1+u}{2u}\Big). \tag{B26}$$

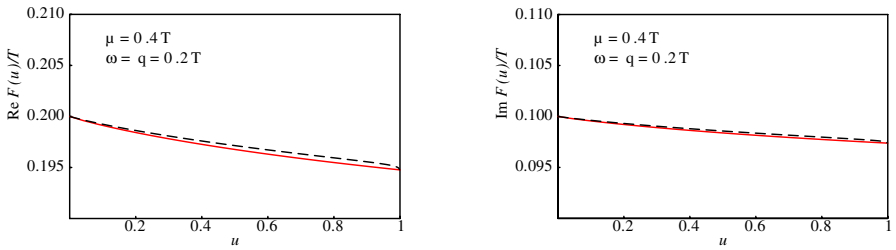

FIG. 3 (color online). These plots show the real and imaginary part of the function $F(u)$ which is part of $X_\alpha = (1-u)^\beta F(u)$. The solid line depicts the analytical approximation, obtained in this paper. As a check we solved the equations of motion for $F(u)$ numerically. They are drawn as dashed lines. In this example we used $T = 1$. The numerical solution was chosen to agree with the analytical one at the horizon and boundary.

3. Solutions for X_3', $\tilde{X}_3'$ and $A_3^{3\prime}$

We give the derivatives of X_3 and $\tilde{X}_3$ as

$$X_3' = -\frac{\mathfrak{w}-\mathfrak{m}}{\mathfrak{q}f}X_0', \tag{B27}$$

$$\tilde{X}_3' = -\frac{\mathfrak{w}+\mathfrak{m}}{\mathfrak{q}f}\tilde{X}_0'. \tag{B28}$$

The solution for $A_3^{3\prime}$ is

$$A_3^{3\prime} = -\tfrac{\mathfrak{w}}{\mathfrak{q}}A_0^{3\prime}. \tag{B29}$$

4. Comparison of numerical and analytical results

As an example, in Fig. 3 we show the numerical and analytical solutions for the function $F(u)$ in $X_\alpha = (1-u)^\beta F(u)$. Here we compare the numerical result for $F(u)$ obtained from the ansatz (3.26) with (3.27) in (3.23) with the analytically obtained approximation given above in (B1) to (B6).

APPENDIX C: ABELIAN CORRELATORS

For convenient reference we quote here the correlation functions of the Abelian super-Maxwell theory found in [2]. The authors start from a five-dimensional supergravity action and not from a Dirac-Born-Infeld action as we do. Therefore there is generally a difference by a factor $N_c/4$. Note also that here all N_f flavors contribute equally. In our notation

$$\begin{aligned} G_{11}^{ab} &= G_{22}^{ab} = -\frac{iN_c^2 T\omega\delta^{ab}}{16\pi} + \cdots, \\ G_{00}^{ab} &= \frac{N_c^2 T q^2 \delta^{ab}}{16\pi(i\omega - Dq^2)} + \cdots, \end{aligned} \tag{C1}$$

$$\begin{aligned} G_{03}^{ab} &= G_{30}^{ab} = -\frac{N_c^2 T\omega q\delta^{ab}}{16\pi(i\omega - Dq^2)} + \cdots, \\ G_{33}^{ab} &= \frac{N_c^2 T\omega^2\delta^{ab}}{16\pi(i\omega - Dq^2)} + \cdots, \end{aligned} \tag{C2}$$

where $D = 1/(2\pi T)$.

APPENDIX D: CORRELATION FUNCTIONS

In this appendix we list the real and imaginary parts of the flavor currents in the first two-flavor directions $a = 1, 2$ and in the third Lorentz-direction coupling to the supergravity fields X_3 and $\tilde{X}_3$ [as defined in (3.21)].

$$\begin{aligned} \mathrm{Re}\, G_{3\tilde{3}}(\omega \geq 0) &= \mathrm{Re}\, G_{\tilde{3}3}(\omega < 0) \\ &= -\frac{N_c q^2(\omega^2 + \mu|\omega|)}{16\pi^2[2\mu|\omega| + q^4/(2\pi T)^2]}, \end{aligned} \tag{D1}$$

$$\begin{aligned} \mathrm{Im}\, G_{3\tilde{3}}(\omega \geq 0) &= -\mathrm{Im}\, G_{\tilde{3}3}(\omega < 0) \\ &= -\frac{N_c T\sqrt{2\mu|\omega|}(\omega^2 + \mu|\omega|)}{8\pi[2\mu|\omega| + q^4/(2\pi T)^2]}, \end{aligned} \tag{D2}$$

$$\begin{aligned} \mathrm{Re}\ G_{3\tilde{3}}(\omega < 0) &= \mathrm{Re}\, G_{\tilde{3}3}(\omega \geq 0) \\ &= -\frac{N_c T(\omega^2 - \mu|\omega|)}{8\pi[\sqrt{2\mu|\omega|} + q^2/(2\pi T)]}, \end{aligned} \tag{D3}$$

and

$$\mathrm{Im}\ G_{3\tilde{3}}(\omega < 0) = 0, \qquad \mathrm{Im}\, G_{\tilde{3}3}(\omega \geq 0) = 0. \tag{D4}$$

APPENDIX E: THERMAL SPECTRAL FUNCTIONS

We include here (Fig. 4) a comparison of the sizes of spectral functions in distinct Lorentz and flavor directions (see also (2.1) in Sec. II).

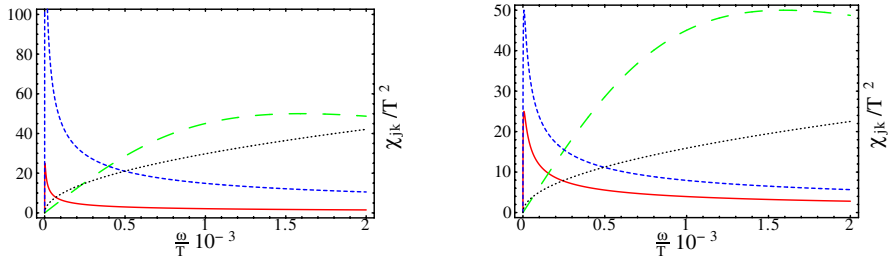

FIG. 4 (color online). Here the thermal spectral functions in distinct Lorentz and flavor directions are plotted against frequency ω/T in units of temperature. In the left plot the chemical potential was chosen to be $\mu/T = 0.7$, in the right one $\mu/T = 0.2$. Both plots were generated with $N_c = 100$. Flavor directions $a = 1, 2$ are summed and displayed as one curve. The frequency-dependence of 00- (solid line) and 03- (short-dashed line) Lorentz directions is shown. By the dotted line we denote the spectral curve in 11- or 22-directions. This curve was scaled by a factor 100 in order to make it visible in these plots. The third flavor direction is only plotted for the spectral function in Lorentz directions 00 (long-dashed curve). We do not show the 33-direction spectral function which has a square-root dependence and is comparable in size with the 11-direction.

[1] G. Policastro, D. T. Son, and A. O. Starinets, Phys. Rev. Lett. **87**, 081601 (2001).

[2] G. Policastro, D. T. Son, and A. O. Starinets, J. High Energy Phys. 09 (2002) 043.

[3] D. T. Son and A. O. Starinets, J. High Energy Phys. 09 (2002) 042.

[4] P. Kovtun, D. T. Son, and A. O. Starinets, J. High Energy Phys. 10 (2003) 064.

[5] P. Kovtun, D. T. Son, and A. O. Starinets, Phys. Rev. Lett. **94**, 111601 (2005).

[6] P. K. Kovtun and A. O. Starinets, Phys. Rev. D **72**, 086009 (2005).

[7] P. Kovtun and A. Starinets, Phys. Rev. Lett. **96**, 131601 (2006).

[8] D. T. Son and A. O. Starinets, J. High Energy Phys. 03 (2006) 052.

[9] J. Mas, J. High Energy Phys. 03 (2006) 016.

[10] K. Maeda, M. Natsuume, and T. Okamura, Phys. Rev. D **73**, 066013 (2006).

[11] A. Karch and E. Katz, J. High Energy Phys. 06 (2002) 043.

[12] M. Kruczenski, D. Mateos, R. C. Myers, and D. J. Winters, J. High Energy Phys. 07 (2003) 049.

[13] J. Babington, J. Erdmenger, N. J. Evans, Z. Guralnik, and I. Kirsch, Phys. Rev. D **69**, 066007 (2004).

[14] M. Kruczenski, D. Mateos, R. C. Myers, and D. J. Winters, J. High Energy Phys. 05 (2004) 041.

[15] T. Sakai and S. Sugimoto, Prog. Theor. Phys. **113**, 843 (2005).

[16] I. Kirsch, Fortschr. Phys. **52**, 727 (2004).

[17] D. Mateos, R. C. Myers, and R. M. Thomson, Phys. Rev. Lett. **97**, 091601 (2006).

[18] T. Albash, V. Filev, C. V. Johnson, and A. Kundu, arXiv:hep-th/0605088.

[19] A. Karch and A. O'Bannon, Phys. Rev. D **74**, 085033 (2006).

[20] K. Kajantie, T. Tahkokallio, and J.-T. Yee, J. High Energy Phys. 01 (2007) 019.

[21] H. J. Schnitzer, arXiv:hep-th/0612099.

[22] K. Ghoroku and M. Yahiro, Phys. Rev. D **73**, 125010 (2006).

[23] K. Ghoroku, A. Nakamura, and M. Yahiro, Phys. Lett. B **638**, 382 (2006).

[24] K. Peeters, J. Sonnenschein, and M. Zamaklar, Phys. Rev. D **74**, 106008 (2006).

[25] C. Hoyos, K. Landsteiner, and S. Montero, J. High Energy Phys. 04 (2007) 031.

[26] D. Mateos, R. C. Myers, and R. M. Thomson, Phys. Rev. Lett. **98**, 101601 (2007).

[27] D. Mateos, R. C. Myers, and R. M. Thomson, arXiv:hep-th/0701132.

[28] R. Apreda, J. Erdmenger, N. Evans, and Z. Guralnik, Phys. Rev. D **71**, 126002 (2005).

[29] R. Harnik, D. T. Larson, and H. Murayama, J. High Energy Phys. 03 (2004) 049.

[30] Z. Guralnik, S. Kovacs, and B. Kulik, J. High Energy Phys. 03 (2005) 063.

[31] J. Erdmenger, J. Grosse, and Z. Guralnik, J. High Energy Phys. 06 (2005) 052.

[32] R. Apreda, J. Erdmenger, and N. Evans, J. High Energy Phys. 05 (2006) 011.

[33] D. Arean, A. V. Ramallo, and D. Rodriguez-Gomez, arXiv:hep-th/0703094.

[34] S. Kobayashi, D. Mateos, S. Matsuura, R. C. Myers, and R. M. Thomson, J. High Energy Phys. 02 (2007) 016.

[35] T. Sakai and S. Sugimoto, Prog. Theor. Phys. **114**, 1083 (2005).

[36] K.-Y. Kim, S.-J. Sin, and I. Zahed, arXiv:hep-th/0608046.

[37] N. Horigome and Y. Tanii, J. High Energy Phys. 01 (2007) 072.

[38] A. Parnachev and D. A. Sahakyan, Nucl. Phys.**B768**, 177 (2007).

[39] C. P. Herzog, A. Karch, P. Kovtun, C. Kozcaz, and L. G. Yaffe, J. High Energy Phys. 07 (2006) 013.

[40] G. Bertoldi, F. Bigazzi, A. L. Cotrone, and J. D. Edelstein, arXiv:hep-th/0702225.

[41] D. R. Reichman and E. Rabani, Phys. Rev. Lett. **87**, 265702 (2001).

[42] E. Rabani, D. R. Reichman, G. Krilov, and B. J. Berne, Proc. Natl. Acad. Sci. U.S.A. **99**, 1129 (2002).

[43] J. K. Bhattacharjee and R. A. Ferrell, Phys. Rev. A **23**, 1511 (1981).

[44] T. X. Liu *et al.*, arXiv:nucl-ex/0610013.

[45] M. B. Tsang *et al.*, arXiv:nucl-ex/0310024.

[46] D. T. Son and M. A. Stephanov, Phys. Rev. Lett. **86**, 592 (2001).

[47] K. Splittorff, D. T. Son, and M. A. Stephanov, Phys. Rev. D **64**, 016003 (2001).

[48] D. Toublan and J. B. Kogut, Phys. Lett. B **564**, 212 (2003).

[49] D. Teaney, Phys. Rev. D **74**, 045025 (2006).

[50] G. Policastro, D. T. Son, and A. O. Starinets, J. High Energy Phys. 12 (2002) 054.